AD-A087 007 NAVAL RESEARCH LAB WASHINGTON DC F/G 19/1
SIMULATIONS OF GAS PHASE DETONATIONS: INTRODUCTION OF AN INDUCT--ETC(U)
JUN 80 E S ORAN, J P BORIS, T R YOUNG
UNCLASSIFIED NRL-MR-4255 SBIE-AD-E000 488 NL

1 OF 1
AD A
087007

END
DATE
FILMED
9-80
DTIC

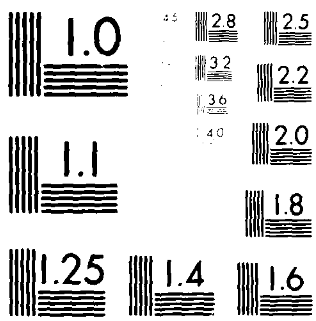
1.0
2.8
2.5
3.2
2.2
3.6
4.0
2.0
1.1
1.8
1.25
1.4
1.6

SECURITY CLASSIFICATION OF THIS PAGE (When Data Entered)

(9) REPORT DOCUMENTATION PAGE		READ INSTRUCTIONS BEFORE COMPLETING FORM
1. REPORT NUMBER NRL Memorandum Report 4255	2. GOVT ACCESSION NO. AD-A087 007	3. RECIPIENT'S CATALOG NUMBER
4. TITLE (and Subtitle) (6) SIMULATIONS OF GAS PHASE DETONATIONS: INTRODUCTION OF AN INDUCTION PARAMETER MODEL.		5. TYPE OF REPORT & PERIOD COVERED Interim report on a continuing NRL problem.
		6. PERFORMING ORG. REPORT NUMBER
7. AUTHOR(s) (10) E.S. Oran, J.P. Boris, T.R. Young, Jr., M. Flanigan, T. Burks*, and M. Picone		8. CONTRACT OR GRANT NUMBER(s) (16) RR024241
9. PERFORMING ORGANIZATION NAME AND ADDRESS Naval Research Laboratory Washington, D.C. 20375		10. PROGRAM ELEMENT, PROJECT, TASK AREA & WORK UNIT NUMBERS 61153N; RR024-241; and 62-0572-0-0
11. CONTROLLING OFFICE NAME AND ADDRESS Office of Naval Research 800 N. Quincy Street Arlington, VA 22203	(11) 25	12. REPORT DATE Jun[redacted] 1980
		13. NUMBER OF PAGES 33
14. MONITORING AGENCY NAME & ADDRESS (if different from Controlling Office) (12) 34 (14) NRL-MR-4255		15. SECURITY CLASS. (of this report) UNCLASSIFIED
		15a. DECLASSIFICATION/DOWNGRADING SCHEDULE

16. DISTRIBUTION STATEMENT (of this Report)

Approved for public release; distribution unlimited.

17. DISTRIBUTION STATEMENT (of the abstract entered in Block 20, if different from Report)

18. SUPPLEMENTARY NOTES

*Present address: Science Applications, Inc., McLean, VA 22101

19. KEY WORDS (Continue on reverse side if necessary and identify by block number)

Detonations
Hydrogen combustion
Methane combustion
Chemically reactive flows

20. ABSTRACT (Continue on reverse side if necessary and identify by block number)

Detailed numerical simulations of supersonic reactive flow and gas phase detonation problems are very expensive due to their computer time and memory requirements. The bulk of this cost is in integrating the ordinary differential equations describing chemical reactions. A global induction parameter model has thus been developed which describes the chemical induction time of a mixture and allows for release of energy over a finite time period. The specific gases for which it has been calibrated are stoichiometric mixtures of hydrogen and methane in air. The relatively inexpensive-

(Continues)

DD FORM 1 JAN 73 1473 EDITION OF 1 NOV 65 IS OBSOLETE
S/N 0102-LF-014-6601

251950 LB

SECURITY CLASSIFICATION OF THIS PAGE (When Data Entered)

20. Abstract (Continued)

induction parameter model is then used in time-dependent one- and two-dimensional simulations of supersonic reactive flows.

CONTENTS

SIMULATIONS OF GAS PHASE DETONATIONS: INTRODUCTION OF AN INDUCTION PARAMETER MODEL

I. Introduction

The recent concentrated effort to understand those factors controlling the detonability of gas mixtures has been triggered by the need to assess hazards related to both LNG spills and containment of material in nuclear power plants. These potentially dangerous situations cover a range of scenarios from unconfined vapor cloud explosions to explosions in partially or totally confined chambers. The materials of concern include mixtures of relatively light weight fuels, such as H_2, CH_4, C_2H_2, etc, in either O_2 or mixtures of O_2 and N_2.

In this paper we describe one- and two-dimensional simulations of gas phase detonations of stoichiometric mixtures of H_2 and CH_4 in air. Primary attention is given to the development and calibration of an induction parameter model to be used in detonation simulations. It will be shown that use of such a calculation to replace the integration of ordinary differential equations representing chemical kinetics extends our ability to do calculations over physically meaningful timescales in air mixtures.

Simulations of gas phase detonation phenomena have been performed by Fickett and Wood[1] using one-dimensional calculations based on the method of characteristics in order to study the stability of the detonation front. These tests were extended to two dimensions by Mader[2] who used several finite difference formulations. All of these calculations, however,

Manuscript submitted April 17, 1980.

assumed a one-step Arrhenius reaction with instantaneous energy release. Taki and Fujiwara[3] used a two-dimensional finite difference method and the two-step reaction model used by Korobeinikov, et al.[4] to simulate detonations in an oxy-hydrogen system. The new contribution presented in this paper is the detailed calibration of an extended induction parameter model by comparison with calculations performed using a detailed computational model which includes a full set of chemical reactions.[5] After benchmark tests are described, the induction parameter model is used in one- and two-dimensional time-dependent simulations of propagating and decaying detonation waves.

II. Summary of the Numerical Models

The reactive shock models used to perform the calculations described below solve the time-dependent conservation equations for mass, momentum and energy.[6,7] In addition, they may solve a set of coupled ordinary differential equations describing the production and loss of a number of chemical species. The convection terms are solved using one variant of the FCT algorithm[8,9] and the ordinary differential equations for the chemical kinetics are solved using a version of the CHEMEQ algorithm.[10,11] An extensive description of the one-dimensional model[5] has shown calculations of incident and reflected shocks in a reactive material. The two-dimensional model has been used to calculate mixing and vortex formation at material interfaces[12] and the effects of the Rayleigh-Taylor instability on the surface of pellets being imploded by lasers.[13,14]

Integration of the chemical rate equations is by far the most expensive part of a reactive shock calculation. Table I summarizes the timing requirements for 2000 timesteps of a detonation simulation performed using the one-dimensional model. Fifty chemical reactions were used to describe the interactions among eight different species. In the calculation of detonation phenomena, we are often interested in whether a particular ignition mechanism with a certain amount of initial input energy will become a self-sustaining detonation. In certain situations, such as H_2-O_2 or CH_4-O_2 mixtures, the characteristic distances out to which a calculation must be performed are a meter or less. In such cases the one-dimensional reactive shock model may be used. If multi-dimensional effects such as cellular structure are to be modelled, the two-dimensional model may be used at great cost. However, for mixtures such as H_2-air and CH_4-air, in which the characteristic distances may be many meters, the computational cost would be exorbitant.

Thus one new addition to both the one- and two-dimensional models is the introduction of a less expensive global induction parameter model to describe the chemical reactions. The required input for this model is a knowledge of the induction time of a mixture as a function of temperature and pressure, $\tau(T,P)$. Then a quantity, $I(\tau)$, is defined which indicates how long the material has remained at a temperature and pressure. This quantity is convected with the fluid in a spatially dependent calculation and it is used to indicate when the available chemical energy should be released. The reaction is <u>not</u> assumed to go immediately to completion. The energy is released over several timesteps determined by the ratio of the sonic transit time to the timestep itself. The basic idea is to keep a whole computational cell from burning at once to eliminate numerical "surging".

The adaptive gridding method discussed by Oran, Boris and Young[5] was generalized for use in the calculations presented below. To illustrate the necessity for varying the spatial gridding adaptively, consider the three temperature profiles shown in Fig. 1. Three different resolution grids were used to perform the same physical calculation, a detailed simulation of a laser-initiated detonation of an H_2-O_2-N_2 mixture. The laser was assumed to have deposited energy by dissociating H_2 or O_2 molecules in a small region at the left hand side. The presence of the radicals quickly triggered chemical reactions and energy release. The raised temperature and pressure then generated a shock wave driven ahead of the flame front.

Since this is a supersonic problem, there is little to be gained from a Lagrangian calculation.[7,23] The velocity of the shock and detonation fronts will be greater than the speed of sound in the unreacted mixture. However, until the sustaining detonation is formed, we are in effect dealing with a flame propagation problem behind a shock front. Thus we must use adaptive gridding to obtain resolution of steep gradients in temperature and species densities. At the short timescales of sonic transit, diffusive transport processes will do little to smooth these gradients.

In order to cope with this problem and achieve the good results shown by the solid curve in Fig. 1, a relatively general adaptive gridding method was developed. As the shock runs out ahead of the flame, one finely zoned region of grid points centers around the shock front and an even finer set centers on the flame front. The location of these regions and the gradual variation of cell size is controlled automatically. Such techniques are a solution to the problem of obtaining the required accuracy while decreasing the number of cells carried in the calculation. A similar technique is used in both the one- and two-dimensional models with which the calculations described below are performed.

III. The Induction Parameter Model

To show how the model for $\tau(T,P)$ is derived, consider Fig. 2 which shows the curves of induction time as a function of initial temperature and pressure for stoichiometric mixtures of hydrogen in air. This has been calculated from the chemical reaction rate scheme constructed and tested by Burks and Oran.[15] In this figure the induction time is chosen to be the time at which the density of the OH radical peaks. This is one way the induction time is defined experimentally.

To be most consistent with the way in which $\tau(T,P)$ is used in the reactive flow model, the induction time should be defined as the time at which the energy of the system begins to increase. This is also the time when the temperature begins to increase rapidly. Figure 3 shows calculations of temperature as a function of time for a stoichiometric CH_4-air mixture at 5 atm which is suddenly heated to temperatures in the range from 1800 to 3000K. The reaction rate scheme used here was derived by Gelinas[17] and has been shown to agree well with measured induction times for stoichiometric mixtures. Noted on these curves is the time of the peak of the atomic oxygen density.

Information such as that summarized in Fig. 2 and shown in more detail in Fig. 3, or well educated estimates if no detailed chemical reaction rate scheme is available, are required as a starting point. We note that for some of the temperatures and pressures characteristic of detonations, there has been no experimental data to compare with the results of the chemical model.

The induction time curves are then fitted to an equation of the form

$$\tau(T,P) = \tau^*(P) \frac{P_o}{P} \exp\left[\frac{A^*(P)}{T-T^*(P)}\right] , \qquad (1)$$

where for convenience P_o = 1 atm. The procedure is to first pick one curve at fixed pressure and guess a value of T*. Then a least squares fit is done to determine the coefficients, $\ell n\, \tau^*$ and A*. These numbers are then used to evaluate Eq. (1). This process is repeated using incremented values of T*, and the final set of values chosen is that set which best reproduces the input data for τ. Calculations are made for a range of pressures from which an analytic form for the coefficients is derived as a function of pressure. Expressions for A*, T*, and $\ell n\, \tau^*$ which give good fits to calculated induction times for stoichiometric H_2-air and CH_4-air mixtures are given in Table II.

These coefficients reproduce induction times determined from chemical model calculations with maximum errors of about 20%. The largest errors occur at low initial temperatures and at pressures greater than five atmospheres. We are also required to specify the energy released from the reactions and this information may be determined from, for example, the JANAF tables.[18]

In the coefficients for both the methane-air and hydrogen-air mixtures, there is a marked change of shape in the coefficients at pressures greater than a few atmospheres. Our analysis of the hydrogen-oxygen chemistry below and above this pressure shows that as the pressure increases, reactions involving HO_2 and H_2O_2 are more important and H_2O becomes important as a reactant. This is consistent with the experimental observations of Voevodsky and Soloukhin[19] and Meyer and Oppenheim[20] who observed this behavior in H_2-O_2 mixtures in the pressure and temperature range above the second explosion limit and below the extended second limit.

Finally, we note that the form of Eq. (1) is similar to that used by both Meyer and Oppenheim[20] and White.[21] In all three cases the form involved an inverse pressure or density dependence and an Arrhenius-type exponential. The addition in Eq. (1) of the temperature offset, $T^*(P)$, in the denominator of the exponential provides another parameter which allows extra flexibility in describing the shape of the induction time curves at higher temperatures. The low temperature cutoff itself does not affect the kinetics in these detonation calculations.

Korobeinikov _et al._[4] and Taki and Fujiwara[3] have given approximations for the amount of energy release and time to equilibration during H_2-O_2 combustion. These approximations and our detailed chemical calculations show that, except at high temperatures, the induction times are generally long compared to the characteristic time for energy release. The energy release timescales are strongly influenced by the time history of the mixture. In detonation problems in which spatial and temporal variations are important, both energy release and induction time modelling are similarly limited in accuracy. Higher order global models could be constructed which depend on characteristics of the time variation of temperature and pressure, but the inaccuracies which occur when data is forced to have a functional form outweigh any expected accuracy gains. From the one-dimensional benchmark comparisons described in the next section we have concluded that local chemical energy release times can be ignored in the induction parameter model.

The simplification proposed above which does not include an energy release time is further supported by previous detonation and reactive shock calculations.[3,5] These show that energy release in a computational cell is governed by the time it takes the deflagration wave to cross the cell dimensions rather than by the energy release time in the relatively thin reaction zone. In the calculations with the induction parameter model presented here, the available chemical energy is released in one acoustic transit time of the cell, which is a good estimate of the transit time of the shock. Furthermore, this approximation ensures a steady progression of the computed reaction zone across the system. In adaptively gridded calculations this acoustic transit time algorithm is particularly important. The computational cells tend to move with the detonation so the effective energy release rate is further reduced from the peak chemical reaction rates.

IV. One-Dimensional Calculations and Benchmark of the Induction Parameter Model

To benchmark the induction parameter model described above and thus determine its accuracy and range of validity, several tests were carried out which compared the results of representative problems solved using the full chemical reaction rate scheme with those solved using the induction parameter model to replace the detailed kinetics. Below we first describe a typical test in some detail and then describe results of other one-dimensional simulations. The reader will appreciate that completely categorizing the behavior and misbehavior of an approximate but complex computational model is an extensive undertaking. Thus not all possible tests are shown or in fact have yet been performed. We hope the reader will become aware of some of the inherent levels of inaccuracy in this kind of calculation from studying the benchmark case presented below. Final solution accuracy of better than 20-30% seems unlikely and much larger errors are possible when dealing with borderline phenomena such as critical detonation and ignition energies. Nevertheless, we present these calculations as the most accurate of the type yet produced for a specific physical system.

The primary benchmark test is a simulation of a bursting diaphragm problem in Cartesian geometry. The driver gas is N_2 and the reactive mixture is a stoichiometric H_2-air mixture at 300°K and 1 atm of pressure. The system was 10 cm long with the diaphragm at 1 cm. The analytic Rankine-Hugoniot solution to the problem indicates that if there were no viscous losses and no chemical reactions, an initial shock of Mach number 4.3 would propagate into the detonable mixture at 1.7×10^5 cm/sec. The temperature and pressure behind the shock front should be 1280°K and 22 atm, respectively.

Figure 4 shows calculations of the maximum temperature in the system as a function of time. The detailed calculation was carried out for 500 steps and the induction parameter model for 3000 steps. The adaptive gridding algorithm used 110 cells with a minimum cell size of 0.006 cm. Also shown on Fig. 4 are comparisons of the position of the shock and detonation front as a function of time. Both of the models show an increase in velocity at about the time that the chemical energy release becomes significant and the differences in these globally determined integral quantities is slight.

Figure 5 shows the temperature as a function of position at steps 300 and 400. Energy release begins in the shocked material which has been heated the longest. Thus a deflagration front is created which moves across shock-heated gas. The rate of propagation of the deflagration is controlled primarily by the induction time of the material. Eventually an equilibrium is reached in which the energy release occurs at some short distance behind the shock front. It can be seen from Fig. 5 that the detailed model reaches this distance slightly sooner than the induction parameter model. By step 400, they have both reached this equilibrium.

Several sources of potential inaccuracy in the global induction parameter model have been discussed earlier. The largest of these we believe to be the intrinsic assumption that $\int_o^t dt/\tau = 1$ implies the onset energy release. This approximation, however, is an improvement to the single Arrhenius-type reaction approximation because it is constructed to be exactly correct whenever the temperature is constant throughout the induction period. As new results and hence improved calibrations become available, improved analytic fits for generalized forms of the model will be made.

The calibrated induction parameter model for H_2-air was next used to investigate the minimum diameter and the associated minimum detonation energy for spherical geometry. The calculations simulated a spherical bursting bubble problem with an N_2 driver gas at 1100°K and about 700 atm of pressure. Tests were performed in which the volume containing the driver gas was increased until a minimum ignition radius for detonation was determined. This corresponds roughly to adding energy to the system until a minimum detonation energy is determined. As shown in Fig. 6, the minimum radius for detonation is between 4.9 and 5.0 cm corresponding to energies between 1.0×10^6 and 1.1×10^6 J. Currently a systematic study using this method for determining minimum energies of ignition is being carried out for H_2-air and CH_4-air mixtures in which the composition of the driver gas and the delivery of the initial added energy are varied.

Several calculations and tests have been performed using the stoichiometric CH_4-air model described in the previous section. Because the induction times for methane systems are always longer than for H_2 systems at equal pressures, temperatures and stoichiometries, the temperature plateau between the shock and burn front is correspondingly longer. Results of two-dimensional simulations which use this model are presented below. Detailed calibrations such as described for the H_2 system are currently being set up for methane and other fuels for which the reaction kinetics are relatively well known.

V. Two-Dimensional Detonation Simulations

Two multi-dimensional calculations of propagating detonations have been performed using the FAST2D computer code.[13,14] Both used the induction parameter model calibrated above for stoichiometric hydrogen-air and methane-air mixtures. Realistic detonations seem to settle into dynamically stable criss-crossing cellular patterns.[24,25,26,27] The essential instability of a planar or near-planar detonation to transverse perturbations has been previously demonstrated by Fickett and Wood[1] and by Mader.[2] Here we are concerned with the nonlinear limit cycle of these transverse perturbations in the given gas mixtures.[3]

The two-dimensional calculations were both performed on a 100 cell by 30 cell Cartesian grid. The system and cell sizes for the methane-air calculation ($\Delta x = 0.15 - 1.5$ cm, $\Delta y = 0.15$ cm) were chosen to be ten times those used for the hydrogen-air calculation. The longer induction times for methane lead to correspondingly longer reaction zones and larger stable detonation cell sizes.[28] To permit spatially extensive calculations, a region of 50 fine zones centered on the shock and driving deflagration are adaptively embedded in a grid of 5C coarse cells. The total system length was 82.5 cm. Solid wall, reflecting, free slip boundary conditions were applied at all four boundaries: x=0 and 82.5 cm, y=0 and 4.5 cm. The result is the two-dimensional planar geometry shown schematically in Figs. 7 and 8.

The system was initialized by assuming that an oblique Mach 5 shock existed in a small region at the left hand end of the tube. The shock front was oriented at 60° from the horizontal x axis, as shown in Fig. 8.

In the shaded region from x=0 to x=1.5 cm, the induction parameter, which satisfies the equation

$$\frac{\partial I}{\partial t} + V_x \frac{\partial I}{\partial x} + V_y \frac{\partial I}{\partial y} = \frac{1}{\tau(T,P)}, \qquad (2)$$

was linearly ramped from 1.2 to 0 to provide a smooth initiation of energy release. I(x,y) was set to zero throughout the remainder of the computational mesh. For the hydrogen-air calculation a Mach 4 shock at 85° was chosen so that we may study the growth of transverse structures which start from the relatively small perturbation shown on the left of Fig. 7A. In both figures the primary shock location is plotted at several different times. The number of computational timesteps is also indicated. The narrow lines behind the primary shock at several of the times show the instantaneous location of dynamic pressure maxima (secondary shocks) in the heated, shocked flow.

In Fig. 7 the hydrogen-air system displays growth of transverse perturbations from a rather small initial amplitude which reach a nonlinear limit cycle by 9.5 μsec. The temperature and pressure increase arising from shock reflection at the upper and lower walls leads to more rapid local chemical energy release. This in turn enhances the reaction rate behind a cylindrically expanding Mach stem which intersects the weakening incident shock. When the Mach stem reaches the other wall, another reflection is generated and the roles of incident shock and Mach stem are interchanged.

When the system size is larger, as in Fig. 7B, a more complex pattern consisting of two detonation cells develops. This indicates that the .45 cm half-width of the upper calculation must be close to the stable free space half-cell size. Taki and Fujiwara[3] mention analogous results for a simplified $H_2:O_2$ system.

Figure 8 shows a similar calculation for the methane-air mixture where the initial shock is given a larger angle from the horizontal to speed attainment of a stable limit cycle. Again the system settles into the single mode fundamental, suggesting that the 4.5 cm half-width is again close to the free space value. In fact, this value agrees qualitatively with Urtiew's estimate.[28] The axial replication length of this pattern is about 18 cm, but this clearly depends on the specified system height, 4.5 cm.

Taki and Fujiwara[3] show that the average propagation rate of the detonation, even in its multidimensional form, is close to the Chapman-Jouguet velocity. This is not surprising, since only global properties of the undisturbed gas are involved. The peak pressure in these two-dimensional calculations fluctuates from a maximum at shock reflection to a value more than a factor of two smaller just before the next shock reflection. This maximum occurs at the triple point and decays continually until the next shock reflection occurs. The characteristic induction distance at the rear of the incident shock just before reflection is much larger than the induction distance behind either of the shocks when the Mach stem is short. Thus this maximum distance must be intimately related to the preferred structural size.

VI. Conclusion

In this paper we have described an induction parameter model for use in detonation and other reactive shock problems. The calibration of this simplified model has been discussed and results have been presented for one- and two-dimensional problems.

The results described show the importance of developing calibrated phenomenological models for use in complex reactive flow problems. Table I clearly shows what may be gained in computational time. However, since the programs required to integrate the ordinary differential equations describing the chemical reactions and all of the information about reaction rates and intermediate species no longer must be stored, a greatly increased system size also can be considered. This is helped by the use of the adaptive gridding techniques mentioned above.

Thus we feel that reasonably reliable calculations may now be performed at relatively little expense for one-dimensional systems that may be meters long. The other gain for multi-dimensional systems is the ability to represent even more complicated chemistries inexpensively by the same procedure. Work is continuing on the preferred cell size problem and the problem of understanding cell regeneration in expanding detonations.

Acknowledgments

This work was sponsored by the Naval Research Laboratory through the Office of Naval Research. The authors would like to thank Professor John Lee, Dr. Paul Urtiew and Dr. Harry Phillips for many helpful and encouraging discussions.

Table I

Computational Information on Benchmark Tests

General Description	Detailed Simulation	Induction Simulation
Number of cells	110	110
Distance simulated	2 cm	2 cm
Minimum cell size	0.006 cm	0.006 cm
Maximum cell size	0.1 cm	0.1 cm
Computer Storage Requirements	80 K bytes[a]	[b]
Timing Breakdown		
Number of timesteps	2000	2000
Typical Timestep	7.7×10^{-9} sec	7.7×10^{-9} sec
Convective Transport	20 sec	14 sec
Chemistry	130 sec	6 sec
Total Time	150 sec	20 sec

a. This includes the full software to do the diffusive transport calculations which are not included in the work described in this paper.

b. The induction parameter model was set up as an option in the full simulation. Eliminating the chemical integration routines would greatly reduce core requirements.

Table II

Induction Time Fits

$$\ln \tau = \ln \tau^* + \frac{A^*}{T-T^*} \quad ; \quad y = \ln P(\mathrm{atm})$$

$$Z = y + 1.25$$

$H_2:O_2:N_2/2:1:4$

$$\ln \tau^* = -\ 14.64 + 1.30Z^2/(6.09+Z^2)$$

$$A^* = 4100 - 3850Z^2/(7.33+Z^2)$$

$$T^* = 300 + 1350Z\ /(18.75 + Z\ )$$

$CH_4:O_2:N_2/1:2:8$

$$\ln \tau^* = -\ 216 + 0.967y + 0.104y^2 - 0.08y^3$$

$$A^* = 2.49\times10^4 - 5.01\times10^3 y - 4.36\times10^2 y^2 + 3.96\times10^2 y^3$$

$$T^* = -\ 184 + 291y + 23.1y^2 - 21.1y^3$$

References

1. Fickett, W. and Wood, W. W. : Phys. Fluids 9, 903, 1966.
2. Mader, C. L. : Twelfth Symposium (International) on Combustion, p.701, The Combustion Institute, 1969.
3. Taki, S. and Fujiwara, T.: AIAA 9th Fluid and Plasma Dynamics Conference, p.1, American Institute of Aeronautics and Astronautics, 1976.
4. Korobeinikov, V. P., Levin, V. A., Markov, V. V., and Chernyi, G. G.: Astronautica Acta 17, 529, 1972.
5. Oran, E. S., Young, T. R., and Boris, J. P.: Seventeenth Symposium (International) on Combustion, p.43, The Combustion Institute, 1978.
6. Williams, F. A.: Combustion Theory, Addison Wesley, 1965.
7. Oran, E. S. and Boris, J. P.: Prog. Energy, Comb. Sci., to appear in 1980.
8. Boris, J. P. and Book, D. L.: Methods in Computational Physics, Vol. 16, p.85, Academic Press, 1976.
9. Boris, J. P.: Flux-Corrected Transport Modules for Solving Generalized Continuity Equations, Naval Research Laboratory Memorandum Report 3237, 1976.
10. Young, T. R. and Boris, J. P.: J. Phys. Chem. 81, 2424, 1977.
11. Young, T. R.: CHEMEQ - A Subroutine for Solving Stiff Ordinary Differential Equations, Naval Research Laboratory Memorandum Report 4091, 1979.
12. Boris, J. P. and Oran, E. S.: International Colloquium on Gas Dynamics of Explosions and Reactive Systems, American Institute of Aeronautics and Astronautics, to appear in 1980.

13. Boris, J. P.: Comments on Plasma Physics and Controlled Fusion, 3, 1, 1977.

14. Bodner, S. E., Boris, J. P. and Cooperstein, G.: Plasma Physics and Controlled Nuclear Fusion, Vol. III, p.17, International Atomic Energy Agency, 1978.

15. Burks, T. and Oran, E. S.: Analysis of the Detailed Chemical Reaction Rate Mechanism for H_2-O_2 Combustion, to appear as a Naval Research Laboratory Memorandum Report, 1980.

16. Oran, E. S. and Boris, J. P.: International Colloquium on Gas Dynamics of Explosions and Reactive Systems, American Institute of Aeronautics and Astronautics, to appear 1980.

17. Gelinas, R. J., Ignition Modelling, Science Applications Report PL-NII-78-02, 1979.

18. Stull, D. R. and Prophet, H.: JANAF Thermochemical Tables, 2nd Edition, National Standard Reference Data Series, U. S. National Bureau of Standards, 1971.

19. Voevodsky, V. V. and Soloukhin, R. I: Tenth Symposium (International) on Combustion, p.279, 1965.

20. Meyer, J. W. and Oppenheim, A. K.: Thirteenth Symposium (International) on Combustion, p.1153, 1970.

21. White, D. R.: Eleventh Symposium (International) on Combustion, p.147, 1967.

22. Phillips, H.: Decay of Spherical Detonations and Shocks, No. 7, British Governments Health and Safety Executive, 1977.

23. Boris, J. P.: Numerical Solution of the Continuity Equation, Naval Research Laboratory Memorandum Report 3327, 1976.

24. Urtiew, P. A.: Acta Astronautica 3, 187, 1976.

25. Lee, J. H. S.: Ann. Rev. Phys. Chem. 28, 75, 1977.

26. Strehlow, R. A.: Astronautica Acta 15, 345, 1970.

27. Strehlow, R. A.: Comb. Sci. Technol. 4, 65, 1971.

28. Urtiew, P. A. and Tarver, C. M.: International Colloquium on Gas Dynamics of Explosions and Reactive Systems, American Institute of Aeronautics and Astronautics, to appear in 1980; also Preprint UCRL-82270, Lawrence Livermore Laboratories, 1979.

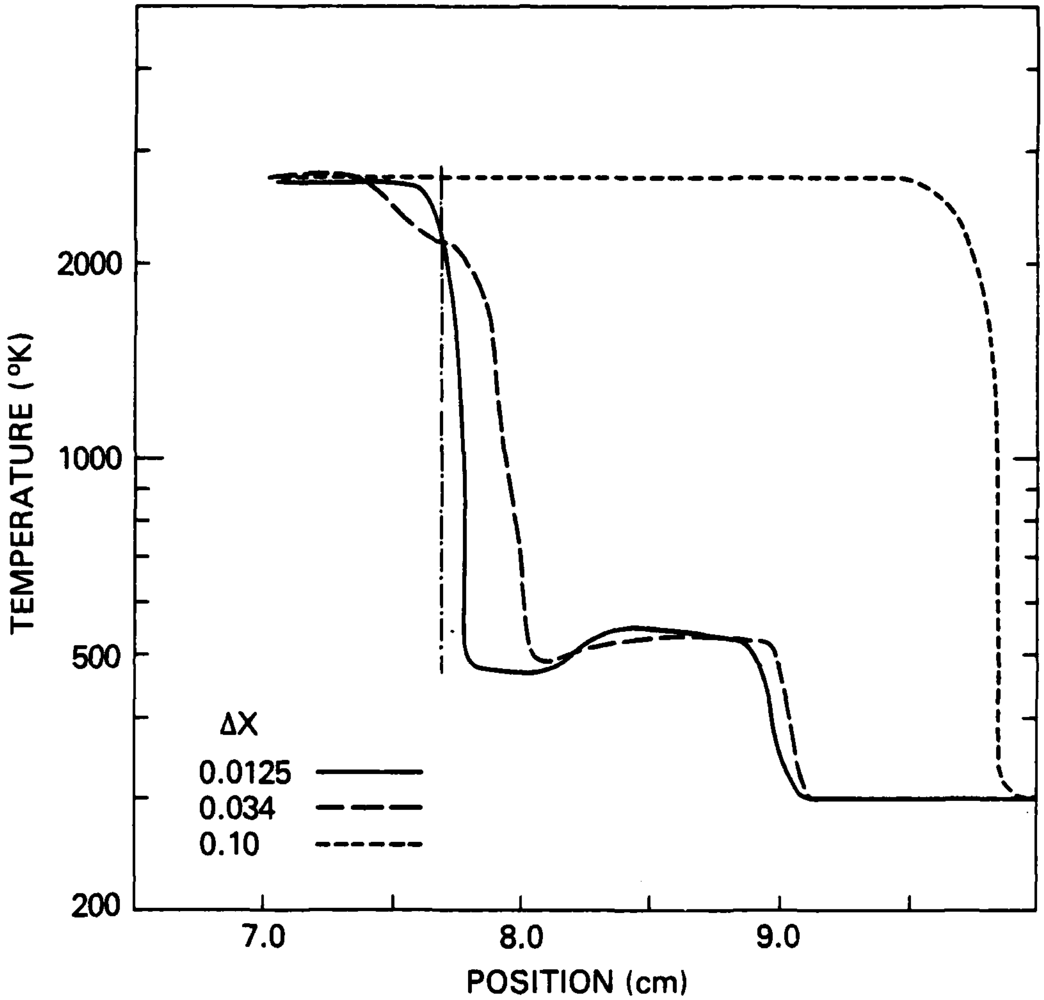

Fig. 1 — Calculations of temperature as a function of position in a laser initiated detonation. Three sizes of computational cells were used giving progressively better resolution. The vertical line indicates the correct position of the burnfront.

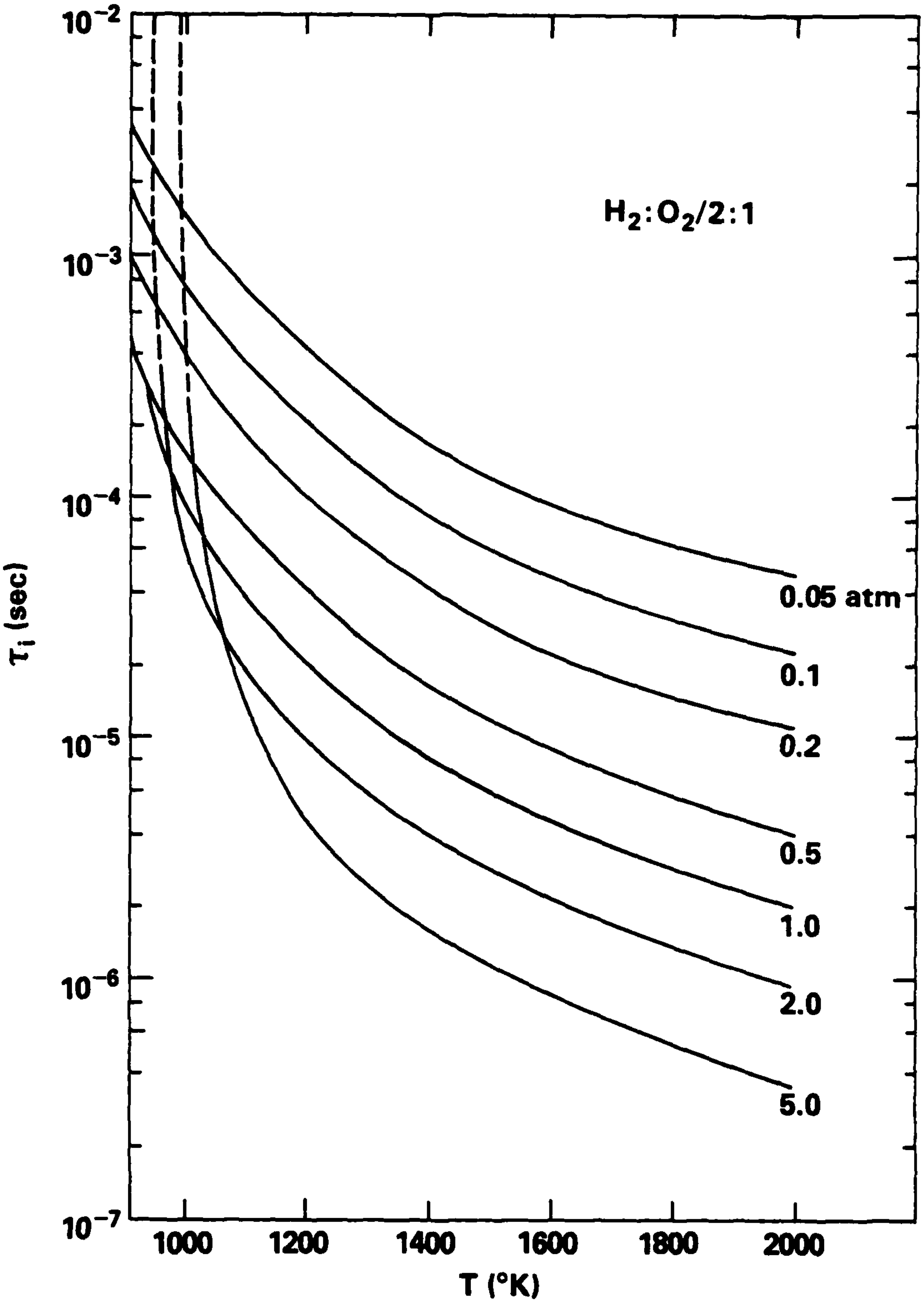

Fig. 2 — Calculated induction times as a function of temperature for various pressures in a stoichiometric H_2-air mixture.

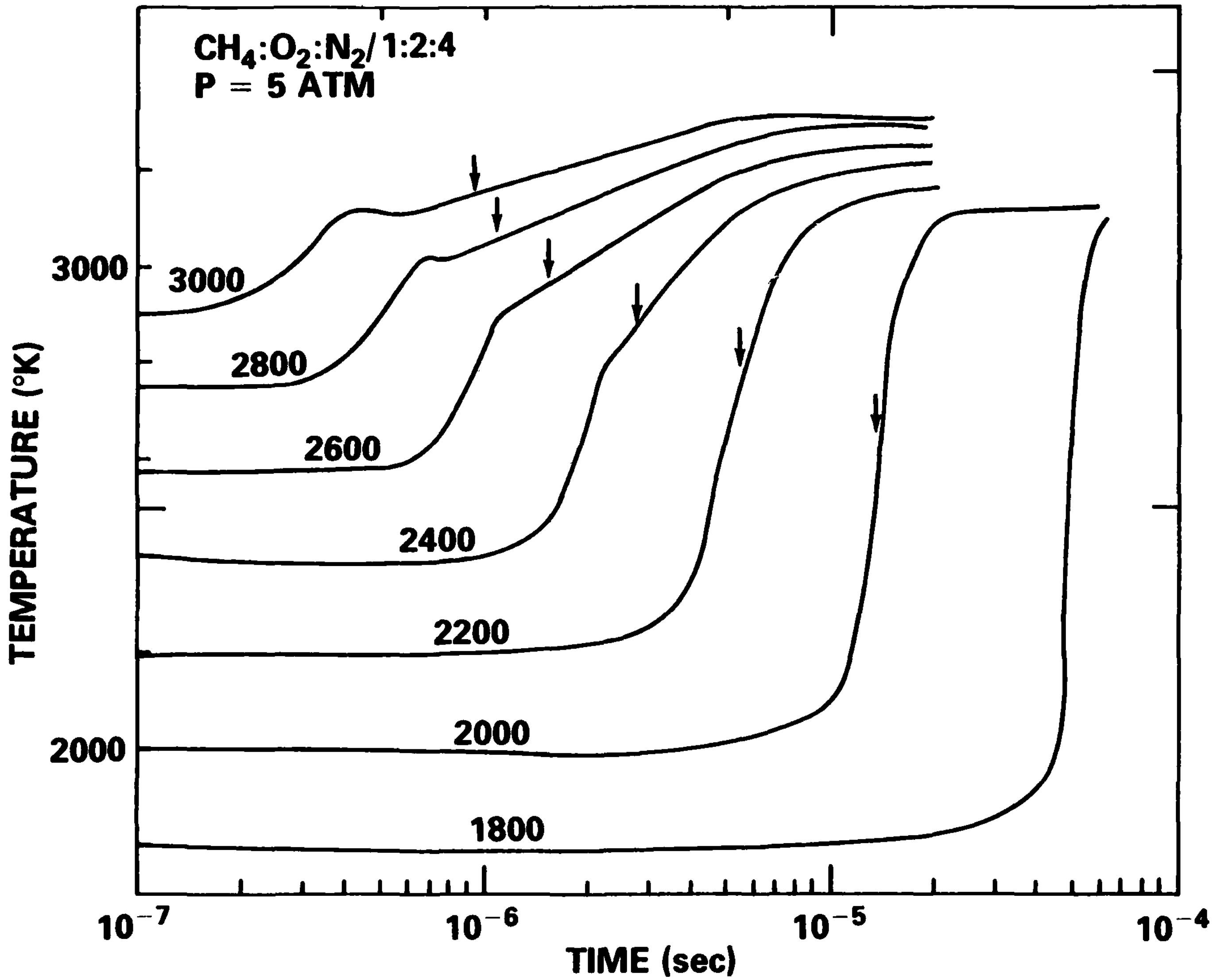

Fig. 3 — Calculations of temperature as a function of time for various initial temperatures at 5 atm in a stoichiometric CH_4-air mixture. The arrows indicate the time of maximum oxygen atom concentration.

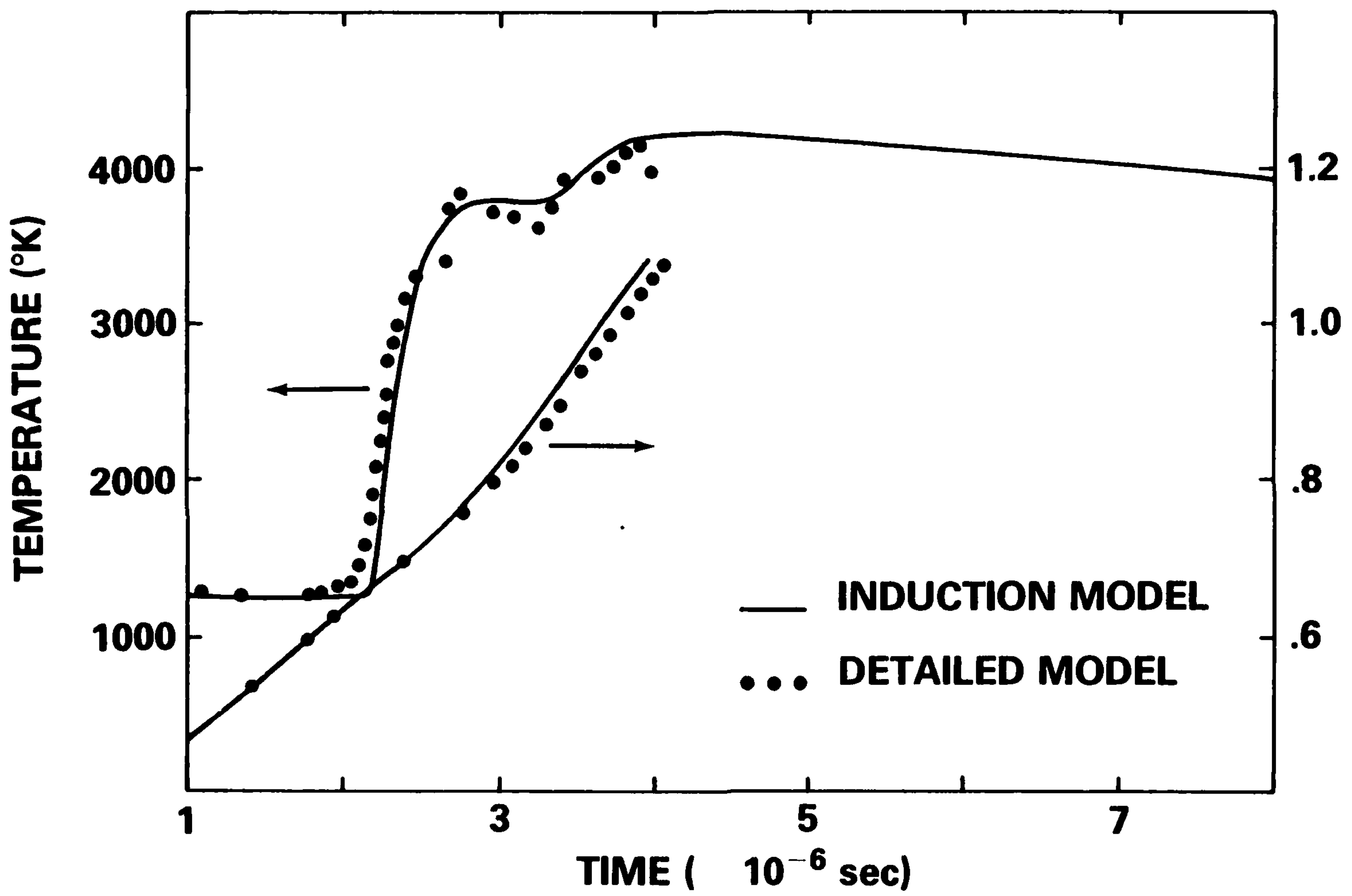

Fig. 4 — One-dimensional calculations of the maximum system temperature and shock front position as a function of time using the induction model (solid and dashed lines) and the detailed model (dots) for the stoichiometric H_2-air system.

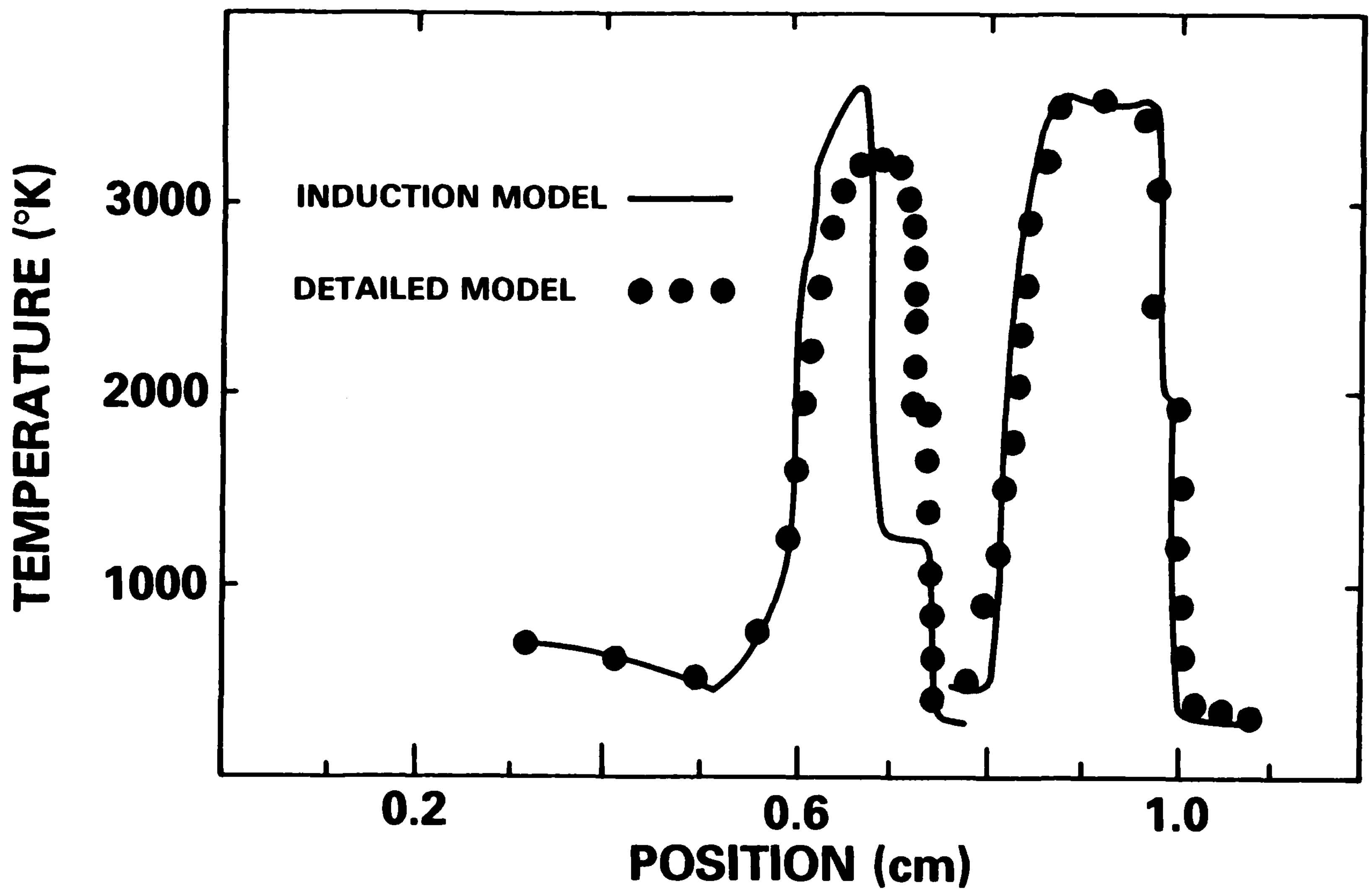

Fig. 5 — Comparison of calculations of temperature as a function of position at steps 300 and 400 for the induction model and detailed calculations.

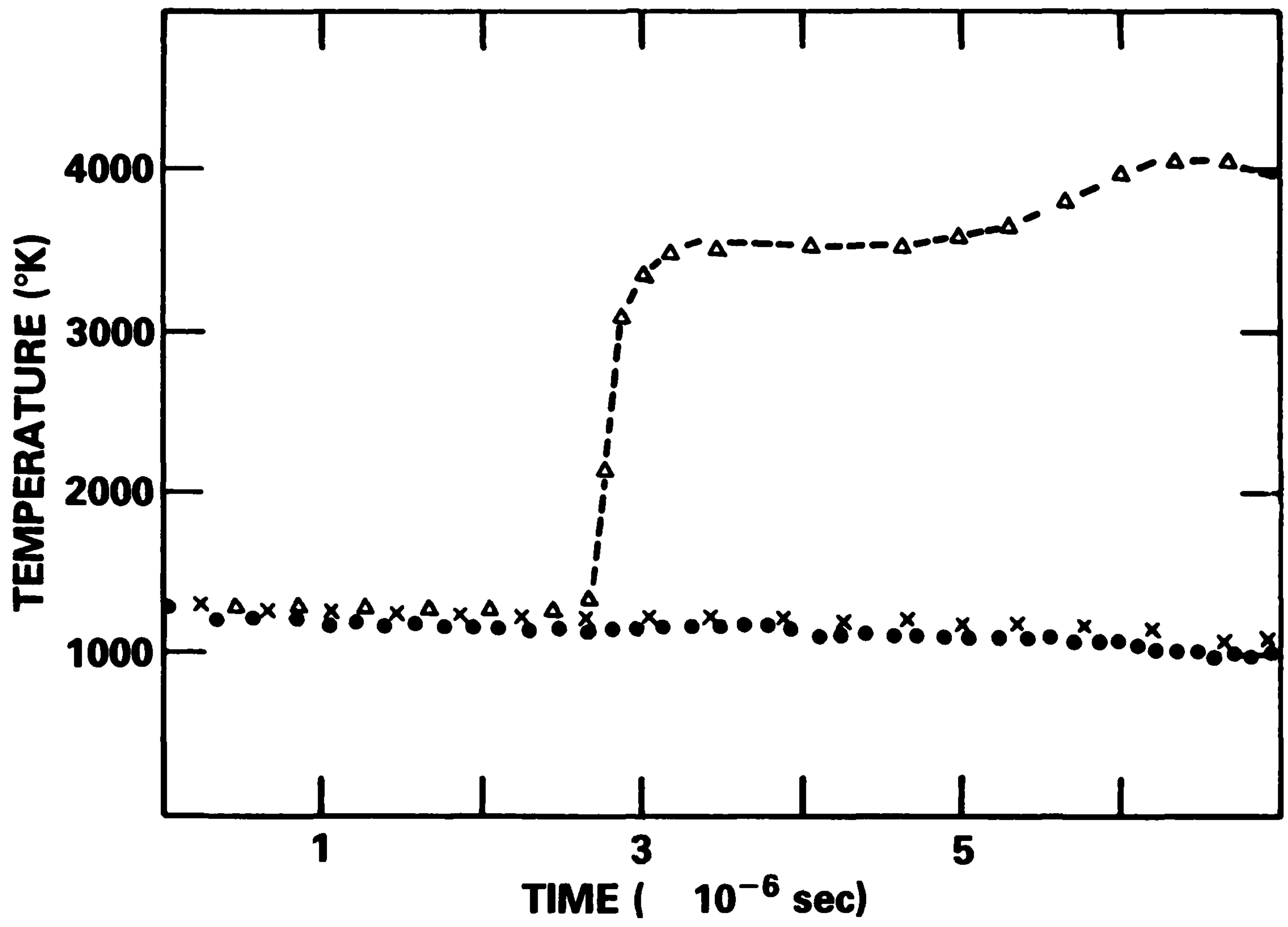

Fig. 6 — Maximum system temperature for three values of the radius of the driver gas in a stoichiometric H_2-air bursting bubble problem. The Δ's correspond to radius = 5 cm, the x's to 4.75 cm, and the ●'s to 4 cm.

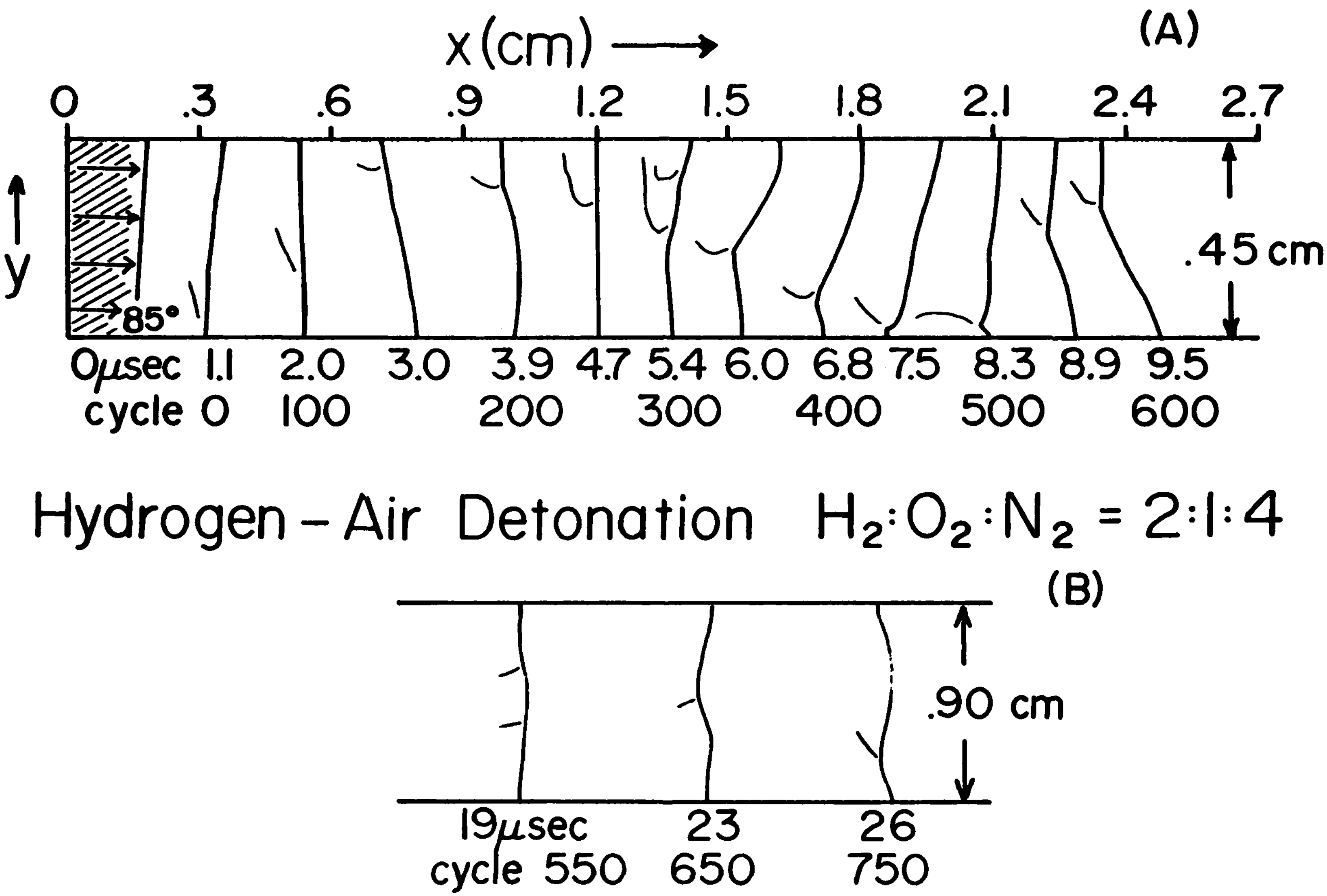

Fig. 7 — Shock front evolution for a hydrogen-air detonation. In narrow channel, (A) .45 cm high, the fundamental cellular pattern develops whereas mode 2 appears in (B) when the channel is twice as high.

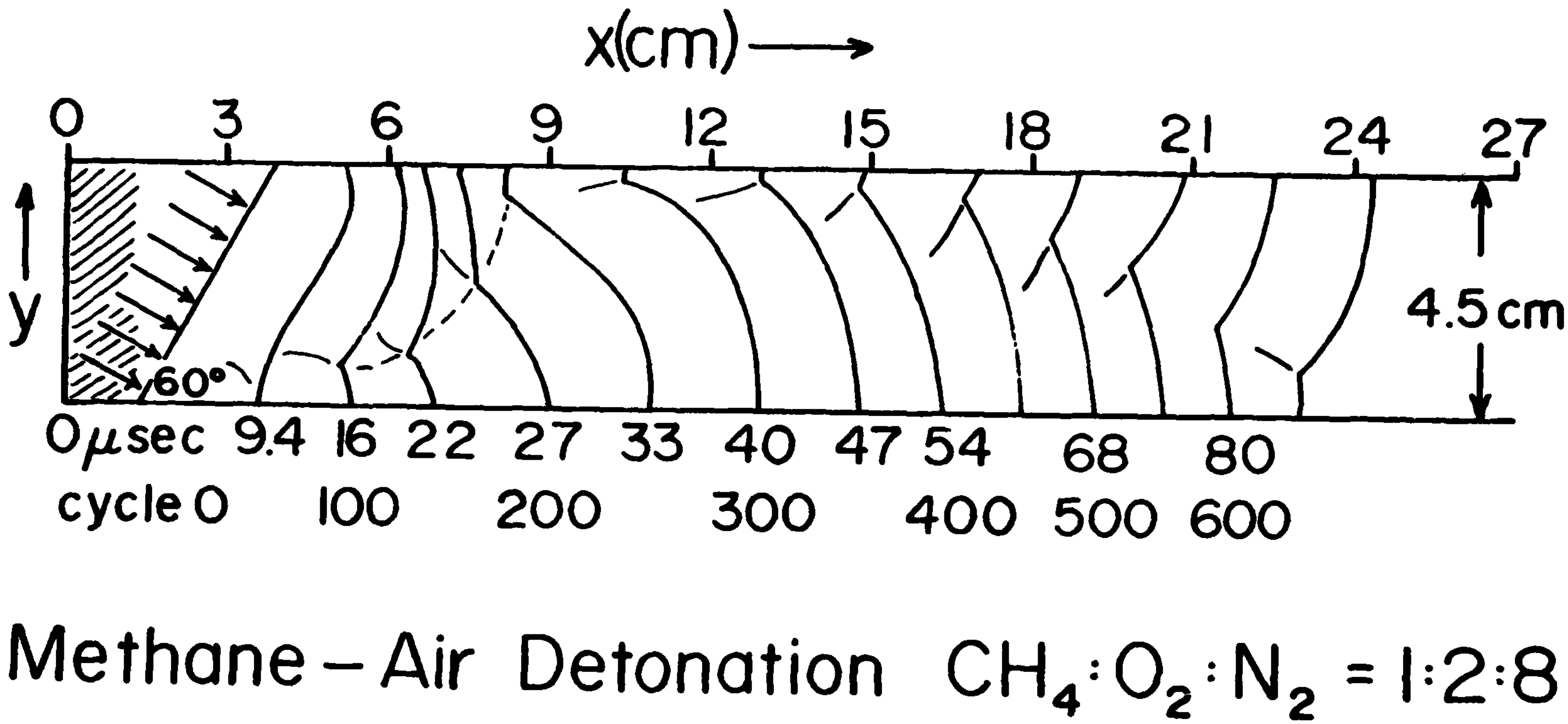

Fig. 8 — Shock front evolution for a methane-air detonation.

FILM

9